

Mechanism of damage, fracture and toughening of TiAl alloys

R.Cao, J.H.Chen

State Key Laboratory of Advanced Non-ferrous Metal Materials, Lanzhou University of Technology , Lanzhou 730050, China, caorui@lut.cn

ABSTRACT: In this paper the authors summarize the results of studies achieved in recent years on the microscopic mechanisms of fracture of TiAl alloys: (1) Cracks prefer to be initiated and propagated along lamellar interfaces, the propagation of crack can take three ways. (2) Mechanism of fracture includes two modes of critical crack triggering fracture and connection of microcracks in the weakest section. (3) Effects of microcrack damage represent the facial effects and the volumetric effects. (4) mechanisms of toughening include: blunting of crack tip, bifurcation of the crack tip, deflection of the crack by lamellae and formation of a diffuse zone of microcracks, stopping the crack at the boundary of a grain with unfavorable orientation or grains and forcing the crack to bypass the barrier grain and take a tortuous path, or cross the barrier grain spending more energy.

KEY WORDS: Cracks, TiAl alloys, Damage, Loading rate, Toughening

In this paper, we summarize our studies in recent years on the mechanism of damage, fracture and toughening of TiAl alloys.

1. Mechanism of crack initiation and propagation

1.1 Crack initiation and propagation

In TiAl alloys, especially in FL alloys, cracks prefer to be initiated and propagated along lamellar interfaces. It is shown in Fig. 1 (crack 1 and crack 2) ([1]).

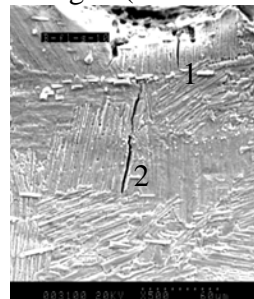


Fig.1 Crack initiation and propagation along the lamellar interface

If there is a barrier made by a grain with a lamellar orientation unfavorable for crack propagation, the propagation of crack can take three ways: (1) a new crack is initiated along the interlamellar interface of a grain ahead of the barrier (Fig. 2(a) ([2])) then the barrier grain is cracked by translamellar cleavage (Fig. 2(b)) ([3]); (2) bypasses the barrier by skipping over the barrier through the grain boundary (Fig. 2 (c)) ([3]); (3) directly crosses the barrier grain by translamellar cracking (Fig. 2 (d)) ([2]).

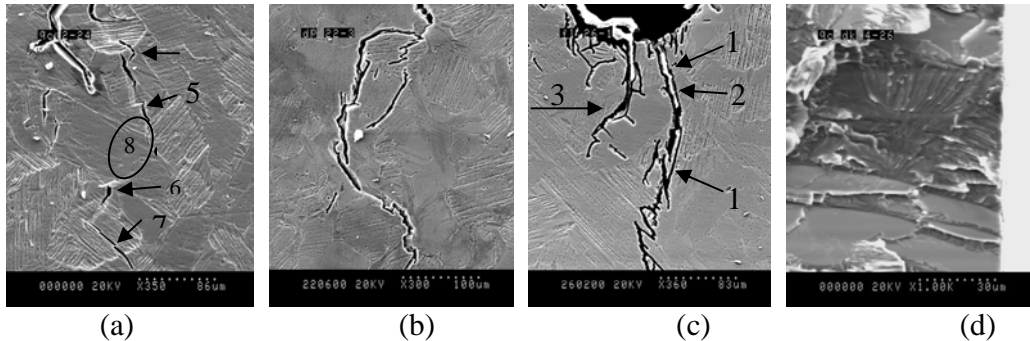


Fig.2 Crack propagation through a barrier grain

1.2 Driving force for crack propagation

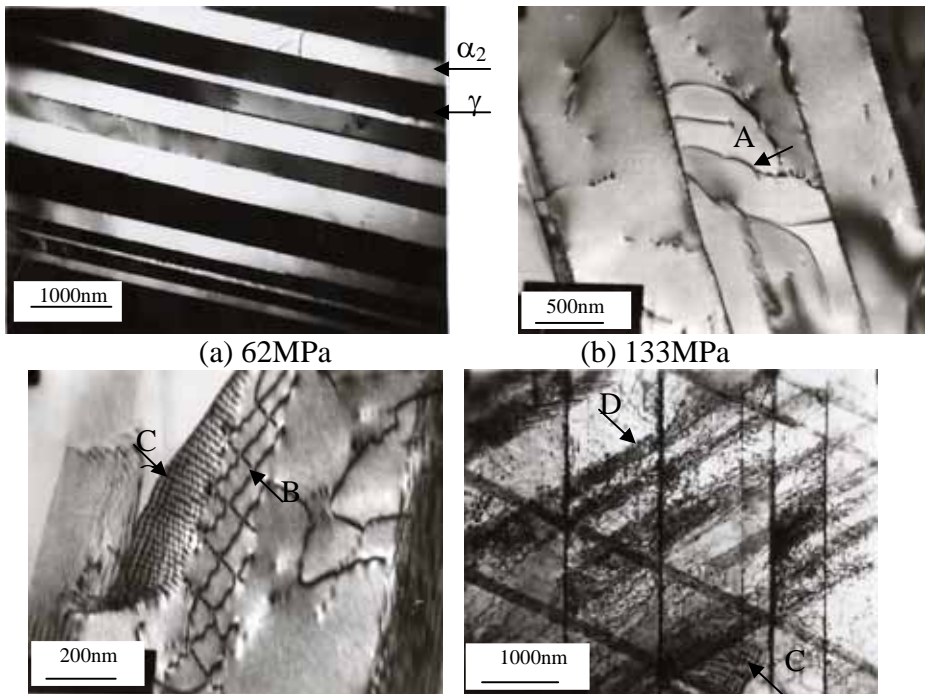
Table 1. Various stresses at the moment of initiation of micro-cracks[2]

Stress	Crack 1	Crack 2	Crack 3	Bifurcated crack	Crack 7	Yield stress ^[4]
σ_{yy} (MPa)	<120	57	109-118	43	60	—
σ_e (MPa)	93	38.7	74-81.8	86.6	75.4	100
τ (MPa)	—	18.4	37-38.2	14.1	39.6	50

σ_{yy} =normal stress to the crack surface, σ_e =equivalent stress at the crack location τ =shear stress acting on the crack

surface, yield stress measured in the soft mode deformation of PST crystal with an angle of 31^0 between the lamellar boundary and the tensile loading axes[4].

Table 1 lists various stresses calculated at the moment of initiation of several microcracks observed in *in-situ* tests. All listed values of stresses initiating crack are lower than the lowest values for inducing yield under the soft mode deformation ($\sigma_e=100$ MPa and $\tau=50$ MPa)[4]. Therefore, cracks are initiated within an elastic environment in a thin tensile specimen. A reasonable inference is that the driving force for initiating a cleavage crack is the tensile stress rather than the shear stress or the plastic strain. *In situ*-observations does not find any slip traces before micro-crack initiation on the surfaces.



(c) 206MPa (d) 339MPa

Fig.3 Images of dislocations produced by various preloads[5]

Fig. 3 shows the images of dislocations produced at various preloading levels [5]. It is seen from Fig. 3, that before the preload reaches 338MPa, the densities of dislocations are low. Nearly no dislocation appears on the metallographic sections of specimen unloaded at $\sigma_{\text{unload}}=62\text{ MPa}$, as shown by Fig. 3(a). In Fig. 3(b), at preload stress=133MPa, few short dislocation lines (shown by arrow A) appear on α_2 phase. In Fig. 3(c), at preload stress=206MPa, typical dislocation net (shown by arrow B) are produced on interface of lamellae are produced within lamellae. In Fig. 3(d), when the preload reached 338MPa, appreciable plastic strain is produced. The dislocation density increases remarkably, and is characterized by dense stacking faults (shown by arrow C) and massive super-dislocation tangles (shown by arrow D).

Fig. 4 shows a schematic Figure comparing the increases of crack density and dislocations with increasing preload. When the applied stress is lower than 338MPa, few dislocations are found, however, appreciable microcracks up to $68/\text{mm}^2$ are observed. It means that in this case most microcracks are not produced by dislocation pileup. Cracking is not necessarily, to be preceded by a plastic strain. In fact, the initiation and propagation of interlamellar cracks can be driven by tensile stress in an elastic environment. Pre-yield cracking during testing in tensile tests was also observed by acoustic emission technology in Ref. [6, 7]. In our work, there is no evidence to support the argument that micro-yield is a necessary precursor for the microscopic cleavage cracking.

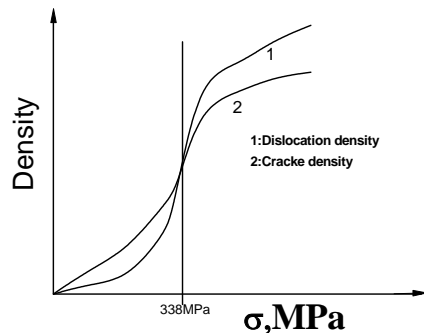


Fig.4 Variations of the crack density and dislocation density with the different preload level σ [5]

2. Mechanism of fracture

2.1 Critical crack triggering-fracture and Damage accumulated-fracture

In tensile tests, fatigue tests, notched bar-bending tests of the fine grain FL TiAl alloys, when a microcrack extends to a critical length which acts as a Griffiths crack and matches the loading stress, the crack propagates catastrophically through entire specimen (Fig. 5) [1]. However for tensile test of the large grain($\sim 1000\mu\text{m}$) FL specimens, a lot of large interlamellar cracks are produced prior to final fracture, which seriously weaken the material. The final fracture happens by

connection of interlamellar cracks on a most damaged section, where the highest density of microcracks is accumulated (Fig. 6) [8].

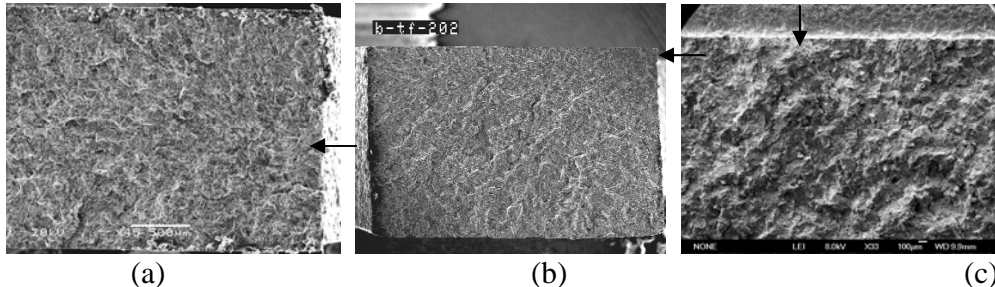


Fig. 5 Fracture triggered by a critical crack in specimens of (a)tensile test, (b)tensile fatigue test and (c) bending tests for fine grain FL alloy [1]

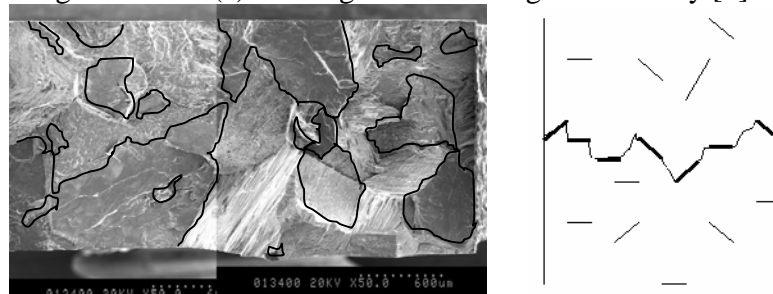


Fig. 6 Fracture surface on a most heavily damaged area of specimens in the tensile tests for large grain FL alloy (1000um)(a) and (b)schematic fracture path of FL microstructure in tensile specimens[8]

2.2 Effects of damage

The damage (microcracks) manifests its effects on producing the critical crack triggering the final fracture. Especially for the fatigue loading case, where the critical crack is a cluster composed of several cracks in different grain colonies, which is formed by repeatedly acting of the fatigue loading to drive the individual crack through the grain boundaries.

Microcrack damage produced the facial effects and the volumetric effects. The volumetric effects induced by microcracks which are produced in entire specimen volume. This Volumetric effect decreases the apparent elastic modulus and causes a stress-softening sector on the load-displacement curve just before final fracture. As shown in Fig. 7, with increasing preload, a trend is presented that the elastic modulus in the subsequent reload (fracture) process decreases. The effects of the microcracks on the reduction of the elastic modulus can be attributed to two factors. The first is that the microcracks reduce the real areas of cross sections of the specimen and increase the real stress on the remaining ligaments of the cross sections. The second is caused by the elongation i.e. by the volumetric effects, of microcrack itself.

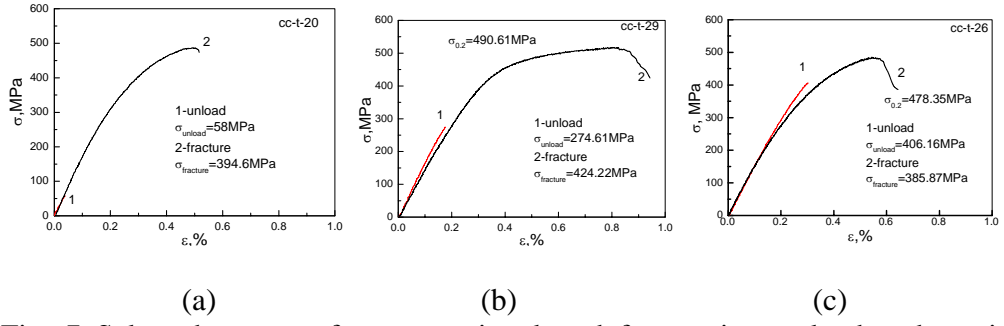


Fig. 7 Selected curves of stress-strain plotted for tension-preload and tension reload processes

For mild steel, this stress-softening sector (Fig7(b)curve 2) is usually caused by an abrupt contraction of the cross section (necking). Because no contraction of cross section has been observed in TiAl specimen, the fast elongation should be also attributed to the volumetric effects of elongation caused by microcracks produced suddenly before the final fracture.

This facial effect of microcrack damage is shown in decreasing the fracture stress. In our preload-reload-unload specimens, in spite of a remarkable variation in the values of the maximum stresses, the stress-softening sectors at the stress-strain curves make most specimens fractured at an applied stress around 400MPa. This value is considered as a minimum value and it corresponds to the maximum crack density which is produced in the processes of preload, reload processes and especially produced in the process which makes the stress-softening sector. From a statistical viewpoint, the maximum fractions of the cross section area occupied by microcracks (i.e. the fractions occupied by weak area on a weakest cross section) are close to each other in various specimens made of the same material. Thus the values of the fracture stresses (defined as the quotient of the fracture load divided by the original section area) for most specimens, which are determined by the remaining area on the cross sections, are distributed around 400MPa and are not affected by the preload process. A supplemental experiment which measured the crack numbers along three cross sections adjacent to the fracture surfaces in three fractured specimens showed that the total microcrack number in each specimen is close to each other. Therefore it is concluded that the fraction of area occupied by the microcracks on a weakest cross section determines the fracture stress of the specimen. This is the facial effect of microcrack damage.

In conclusion, when a displacement-controlled tensile test is performed at a lower strain speed, the effects of microcrack-damage can be summarized as: The volumetric effects which weaken the material by reducing the elastic modulus and produce a stress-softening sector in load-displacement curve and the facial effects which decrease the area of the cross section and the final fracture stress of specimen.

2.3 Effects of loading rate

Because the formation of the critical crack shows a time-delay characteristic, the higher the loading rate, the shorter the critical crack, the higher the tensile strength and vice versa.

Fig. 8 show that in general with lowering the loading rate the tensile strength and ductility (including σ_{uts} , σ_f and ε_f) decrease. Fig. 9 shows the mechanism of reduction of fracture stress, For FL specimens tensile-tested by load-control mode, with lowering the loading rate, the quantity of interlamellar cracks enveloped by blank lines area increases. Because these interlamellar cracks are considered to be produced in the loading process prior to the final fracture, they heavily reduce the cross section and the fracture stress. In Fig. 9(a) specimen was tested at the highest loading rate of 2×10^5 N/min and had a corresponding highest fracture stress of 398 MPa. On the fracture surface, the areas occupied by interlamellar cracks produced prior to final fracture are much less than that on the fracture surface of specimen loaded at a rate of only 20 N/min (Fig. 9(b)), which shows a lowest fracture stress of only 252 MPa.

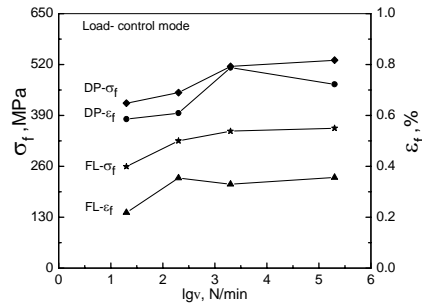


Fig.8. Relationships between the loading rate and mechanical parameters of TiAl-based alloys[8]

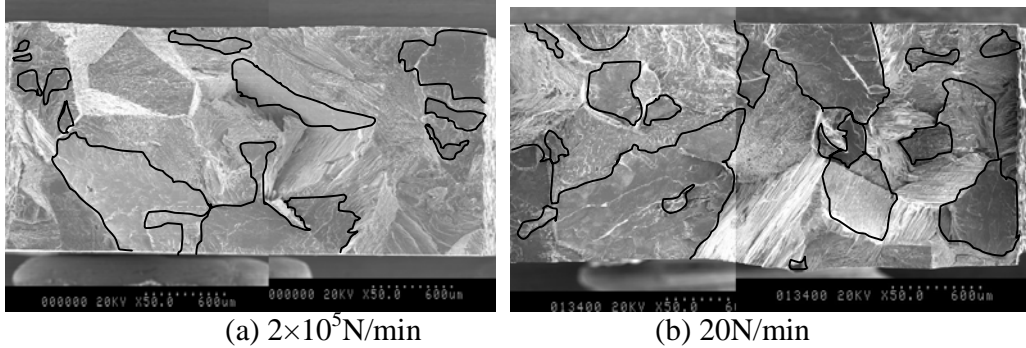


Fig.9. Fracture surface of FL microstructure at the fastest load rate (a) and slowest load rate (b) [8]

At a high loading rate due to the rate-dependent character, less lamellar cracks are produced and connected, and the final fracture was triggered by a smaller interlamellar crack area at a high fracture stress. At a low loading rate, there was sufficient time for lamellar crack production and connection. Final fracture was triggered by a larger interlamellar crack area at a low fracture stress.

For FL specimens 3PB testes, at the lowest rate of 0.00075 mm/min, more interlamellar crack facets are found on the fracture surface, especially in front of the notch root. The main crack takes a more tortuous path for propagation (Fig.10 (a)) and shows a more rough fracture surface. Based on these observations, the following mechanism of loading rate effect is suggested. At a lower loading rate, more lamellar cracks are produced in the grains with the favorite lamellae

orientation even though these grains locate a distance from the centerline of the notch. It means that at a lower loading rate, the time is sufficient to allow lamellar cracks developed in the vicinity (rather than just in front) of the notch root, and to allow the main crack propagated through a more tortuous but low resistance path, which makes the P_{max} lower. In other words, the main crack takes an easy way bypassing grains with non-favorite orientation (lamellae orientation inclined with a larger angle to the direction of main crack). The specimen will be fractured at a lower load P_{max} . At a high loading rate, the time is insufficient to allow interlamellar cracks fully developed, the main crack takes the way along with the centerline through some grains with non favorite orientation (schematically shown by the translamellar cracks in Fig. 10(b)). The specimen will be fractured at a higher load. This is the reason why the fracture toughness of FL alloy increases with increasing loading rate.

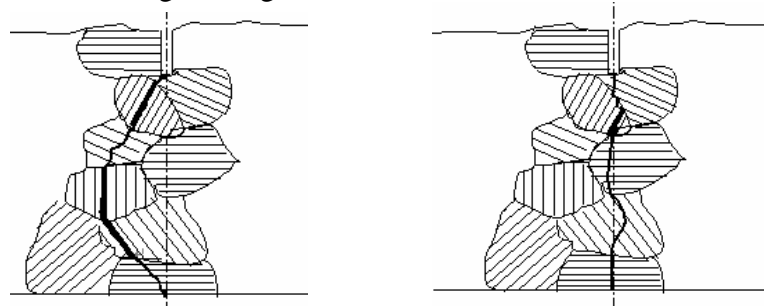


Fig.10. Schematic fracture path of FL microstructure in (a) 3PB specimen at slower loading rate,(b)3PB specimen at higher loading rate[8]

3. Mechanism of toughening

3.1 Reason of the increase of applied load with extending crack length

Because the driving force for the crack propagation is the normal stress, a constant stress should be kept at the extending crack tip. The main crack observed on the surface does not extend all the way through the thickness. The increase of the normal stress caused by the decrease of the ligament area with extending the crack is insufficient to make up the necessary increment for keeping a constant stress at an extended crack tip. The applied load should increase to keep a constant stress-front moving ahead with the extending of the crack in a notched specimen.

3.2 The main toughening mechanisms

Deflection of main crack from the direction of the normal stress is shown in Fig. 11(a). This deflection results from the large lamellae oriented in a large angle declined to the centerline and makes the really acting normal stress lower. Due to the larger interlamellar cracks developed in various directions from the crack tip (shown by many interlamellar crack facets in front of the notch tip, the main crack tip is seriously bifurcated in Fig. 11 (b). In this case the driving force is much less than that in front of an integrated sharp crack. Fig. 11 (c) shows the typical cracks observed in an unloaded FL specimen with blunted tips, which is much wider than that observed in steels tested at low temperatures. The crack tips seem to be blunted by slip of the lamellae along the grain boundary instead of by plastic

strain inside the grain. Formation of a diffused zone of micro-cracks (Fig. 11 (d)) reduces the stress triaxiality around the main crack and disperses the tensile stress. In summary, all mechanisms are related to the lamellar structure of FL microstructure, which could be thought as a composite consisting layers of more plastic γ sandwiched by layers of harder α_2 . The interlamellar strength is very low, but the translamellar strength is much higher than the interlamellar strength. The lamellar structure with different strength in trans- and inter-lamellar directions can make the crack deflect, bifurcate, blunt and produce defused zones of microcracks. These phenomena reduce the driving force for crack extending, and make the main crack difficult to propagate or cause it to be stopped, thus increase the fracture toughness. It is the reason why the fully lamellar structure is used in growth. Therefore, The main toughening mechanisms in FL specimens are deflection of the main crack, bifurcation of the main crack tip, blunting of the crack tip and formation of a diffuse zone of microcracks (Fig. 11(a), (b), (c), (d)) [2].

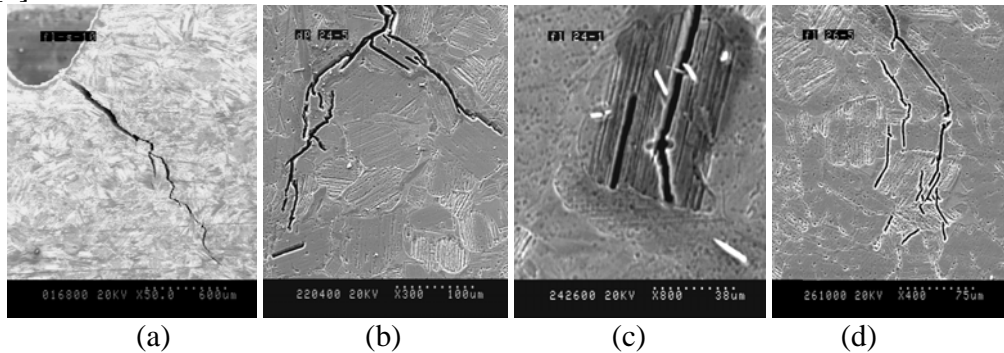


Fig. 11 Mechanism of toughening[2]

An interesting point for another fully lamellar microstructure specimen is that a series of cracks with ligament bridges formed in front of the main crack during crack propagation as shown in Fig. 12. Figs. 12(a-c) show the process of connection of the main crack with these cracks by tearing the ligament bridges. The fracture surface shows the series of cracks and the torn ligaments, these surface ligaments are only $20\mu\text{m}$ - $50\mu\text{m}$ in thickness, which do not afford to offer high resistance to the crack extension. According to a widely accepted argument this process will contribute as a type of extrinsic toughening, i.e. the shear ligament toughening. However, as seen at the crack resistance curve of this specimen in Fig. 12(d), once the series of cracks formed, the applied stress for crack propagation successively decreased despite the deformation and tearing of the ligament bridges. This work, therefore, does not support the idea of shear ligament toughening, because, as a whole, the process of a series of new crack nucleation with a series of ligament bridges formations decreases the crack propagation resistance rather than increases it.

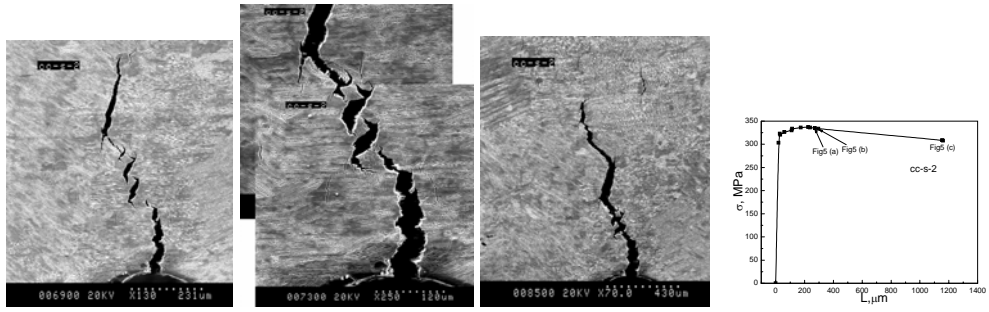


Fig.12 Surface patterns showing the connection of main crack with series cracks by tearing ligament bridges(a-c) and Curves plotting applied stress σ against the lengths of main cracks L(d) [9]

4.Summary

- (1) Cracks prefer to be initiated and propagated along lamellar interfaces. If there is a barrier made by a grain with a lamellar orientation unfavorable for crack propagation, the propagation of crack can take three ways. In tensile tests, fatigue tests, notched bar-bending tests of the fine grain FL TiAl alloys, when a crack extends to a critical length which acts as a Griffiths crack and matches the loading stress the crack propagates catastrophically through entire specimen. However for tensile test of large grain FL specimens, the final fracture happens by connection of interlamellar cracks on a section.
- (2) The initiation and propagation of interlamellar cracks can be driven by tensile stress.
- (3) Effects of microcrack damage present the facial effects and the volumetric effects, the volumetric effects which weaken the material by reducing the elastic modulus and produce a stress-softening sector in load-displacement curve and the facial effects which decrease the area of the cross section and the final fracture stress of specimen.
- (4) The main toughening mechanisms in FL specimens are deflection of the main crack, bifurcation of the main crack tip, blunting of the crack tip and formation of a diffuse zone of microcracks.

References

- [1] R. Cao, Y.Z. Lin, D. Hu, J.H. Chen, Fracture behaviors of a TiAl alloy under various loading modes, Eng. Frac. Mech, 75(15)(2008) 4343-4362.
- [2] J.H.Chen, R.Cao, G.Z.Wang, J. Zhang, Study on Notch Fracture of TiAl Alloys at Room Temperature Metall.Mater.Trans.A, 35A(2) (2004)439-457.
- [3] J. H. Chen, R. Cao, G. Z. Wang, J. Zhang, Fracture behaviour of precracked specimens of a TiAl alloy, Mater Sci & Tech, 21(5)(2005)507-516.
- [4] H. Inui, M. H. Oh. A Nakamura, M Yamaguchi, Room-temperature tensile deformation of polysynthetically twinned (PST) crystals of TiAl, Acta Metall. Mater, 40(1992) 3095-3104.
- [5] R. Cao, H. Zhu, J.H. Chen, J. Zhang, H.J. Yao, Effects of Microcrack-Damage on Fracture Behavior of TiAl Alloy, Part I Displacement-Controlled Tensile Test, Mater Sci & Eng,474(1-2) (2008)1-14.
- [6] X.Wu, D.Hu, R.Botten, M.H.Loretto, The significance of acoustic emission during stressing of TiAl-based alloys. Part II: Influence of cracks induced by pre-stressing on the fatigue life, Acta Mater. 49(10) (2001)1693-1699.
- [7] R.Botten, X.Wu, D.Hu, M.H.Loretto, The significance of acoustic emission during stressing of TiAl-based alloys. Part I: Detection of cracking during loading up in tension, Acta Mater. 49(10) (2001)1687-1692.
- [8] R.Cao, M.X. Lei, J.H. Chen, J.Zhang, Effects of loading rate on damage and fracture behavior of TiAl alloy, Mater Sci & Eng, A465(1-2) (2007) 183-193.
- [9] R.Cao, H.J.Yao, J. H. Chen, J. Zhang, On the mechanism of crack propagation resistance of fully lamellar TiAl alloy, Mater Sci & Eng, A420 (2006)122-134.